News from the CTEQ-TEA collaboration

Marco Guzzi

On behalf of the CTEQ-TEA collaboration

MANCHESTER 1824
The University of Manchester

C T E Q

Epiphany 2017 Conference
Cracow 9-12 January 2017

Intro

Investigation of the structure of the nucleon is crucial for a multitude of high-energy physics programs.

Interpretation of experimental measurements at hadron colliders relies on the precise knowledge of fundamental QCD parameters

and

Parton Distribution Functions (PDFs) of the proton…

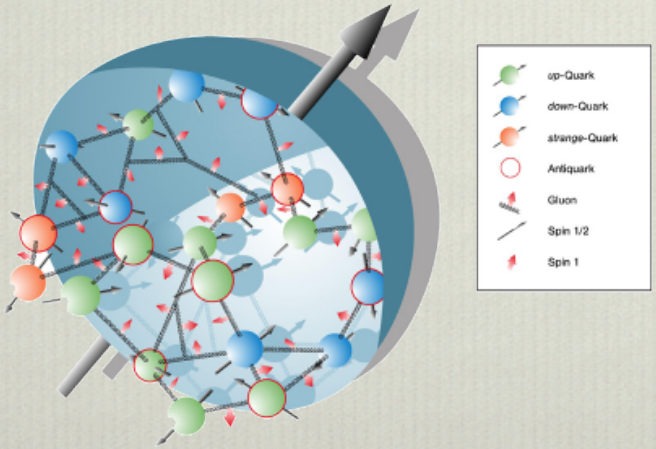

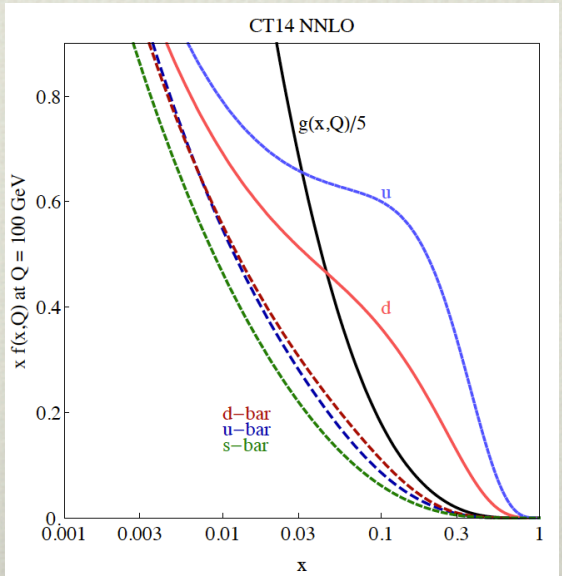

CT14, PRD2016

Collinear PDFs are (universal) complicated objects

they cannot be fully calculated in pQCD,
but are determined by global analyses of world data
using a variety of analytical and statistical methods.

For this reason PDFs are "data-driven" quantities.

Their accuracy must match the accuracy of hard scattering cross section…

…they still represent one of the major sources of uncertanty in theory predictions and simulations at hadron colliders…

Huge efforts currently going on to reduce PDF errors

Unpolarized collinear PDFs at LO, NLO, NNLO in QCD:

Recent (2014-2015) determinations including LHC run I data:

- CTEQ TEA $\Longrightarrow$ CT10, CT14 (Hessian method)
- MMHT $\Longrightarrow$ MSTW, MMHT14 (Hessian method)
- NNPDF $\Longrightarrow$ NNPDF3.0 (MC sampling and neural networks)
- ABM $\Longrightarrow$ ABM12LHC (Hessian method); **ABMP (2016)**

Other recent determinations not including LHC data

- HERA2.0 (Hessian method)
- CTEQ-Jlab $\Longrightarrow$ CJ12 fit (Hessian method)
- JR (Hessian method)

In the past years, a lot of efforts have been put in organizing a sistematic library to access all PDFs with an organic C++ interface:
`https://lhapdf.hepforge.org/`

Extremely important tool for hadron collider phenomenology.

Different methodologies

Methodologies for PDF determination vary among recent PDF analyses:

- smaller/larger/different data sets considered,
- heavy-flavor treatment (GMVFN, FFN,),
- different values/treatment of $\alpha_s(M_Z)$,
- different parametrizations for input PDFs at Q_0,
- ....

$\Rightarrow$ differences in central predictions and error estimate

2012

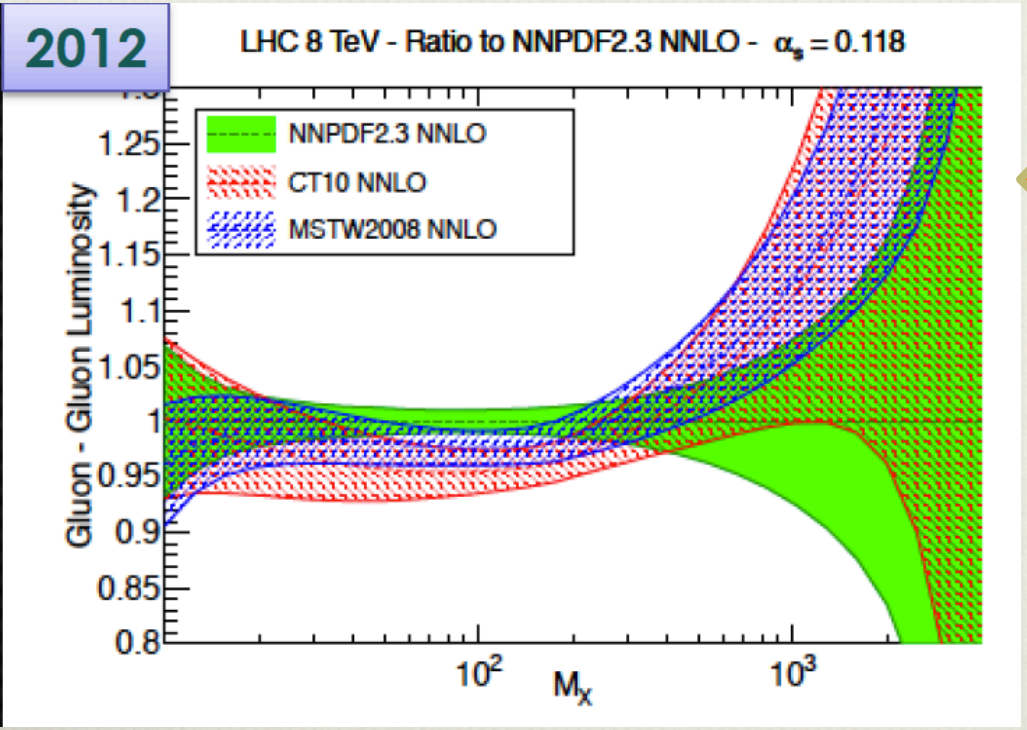

LHC data have little impact in recent global analyses.

A lot of efforts in the past 2 years went into comparisons and benchmarking: "PDF4LHC recommendations for LHC run II", arXiv: 1510.03865

2015

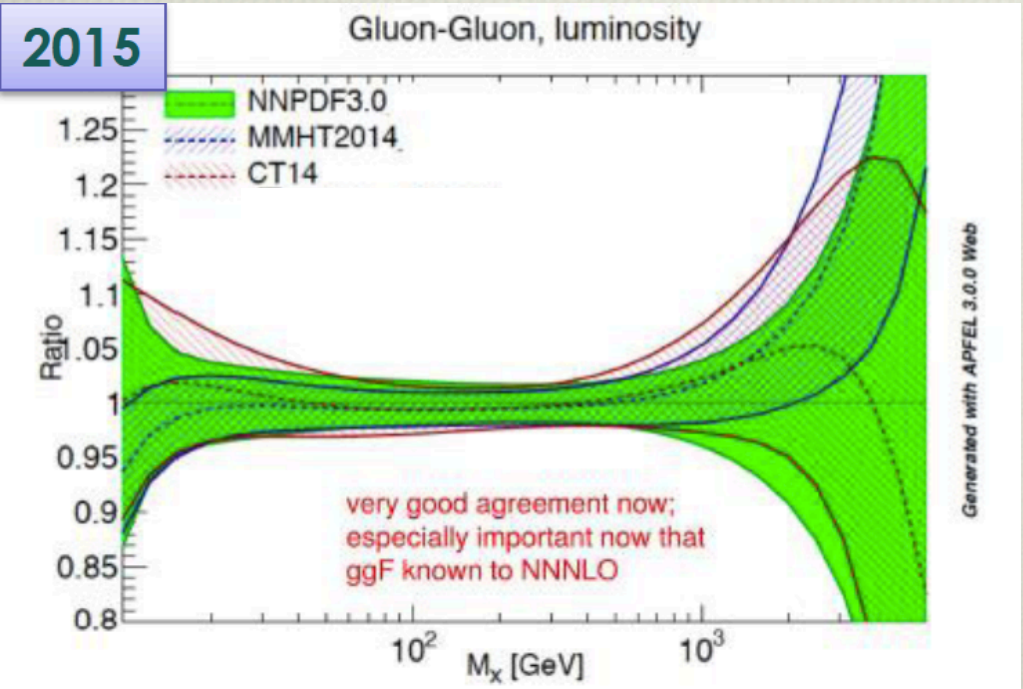

Comparison of PDFs at $Q^2 = 10^2$ GeV^2 between the NNPDF3.0, CT14 and MMHT14 sets at NNLO, with $\alpha_s(M_Z) = 0.118$.

From PDF4LHC arXiv: 1507.00556 (July 2015)

The CT14 global QCD analysis

A quick recap

S. Dulat, T.J. Hou, J. Gao, M. Guzzi, J. Huston, P. Nadolsky,
J. Pumplin, C. Schmidt, D. Stump, C.-P. Yuan

arXiv:1506.07443, PRD2016

TEA group: W.-K.Tung Et Al.

C T E Q

The Coordinated Theoretical-Experimental project on QCD

What's new in CT14 NNLO PDFs

CT14 differs from CT10 PDFs in several respects:

pre-LHC

new HERA data:

- Combined HERA charm production measurements ($F_2^{(c)}$)
- measurements of the longitudinal $F_L(x, Q^2)$ in DIS neutral currents

new Tevatron data:

- Tevatron Run 1 CDF and D0 inclusive jet data are dropped,
- old D0 data (0.75 fb^{-1}) superseded by the new D0 (9.7 fb^{-1}) W-electron rapidity asymmetry data.

LHC 7 TeV run I data included

- ATLAS and LHCb W and Z production,
- ATLAS, CMS and LHCb W-lepton charge asymmetry,
- ATLAS and CMS inclusive jet data.

CT14 has ≈3000 data points

CT14 Data sets ensemble I

ID#	Experimental data set	N_{pt}	χ^2_e	χ^2_e/N_{pt}	S_n
101	BCDMS F_2^p	337	384	1.14	1.74
102	BCDMS F_2^d	250	294	1.18	1.89
104	NMC F_2^d/F_2^p	123	133	1.08	0.68
106	NMC σ^p_{red}	201	372	1.85	6.89
108	CDHSW F_2^p	85	72	0.85	-0.99
109	CDHSW F_3^p	96	80	0.83	-1.18
110	CCFR F_2^p	69	70	1.02	0.15
111	CCFR xF_3^p	86	31	0.36	-5.73
124	NuTeV $\nu\mu\mu$ SIDIS	38	24	0.62	-1.83
125	NuTeV $\bar{\nu}\mu\mu$ SIDIS	33	39	1.18	0.78
126	CCFR $\nu\mu\mu$ SIDIS	40	29	0.72	-1.32
127	CCFR $\bar{\nu}\mu\mu$ SIDIS	38	20	0.53	-2.46
145	H1 σ_r^b	10	6.8	0.68	-0.67
147	Combined HERA charm production	47	59	1.26	1.22
159	HERA1 Combined NC and CC DIS	579	591	1.02	0.37
169	H1 F_L	9	17	1.92	1.7



Very important for PDF determination

CT14 Data sets ensemble II

ID#	Experimental data set	N_{pt}	χ^2_e	χ^2_e/N_{pt}	S_n
201	E605 Drell-Yan process	119	116	0.98	-0.15
203	E866 Drell-Yan process, $\sigma_{pd}/(2\sigma_{pp})$	15	13	0.87	-0.25
204	E866 Drell-Yan process, $Q^3 d^2\sigma_{pp}/(dQdx_F)$	184	252	1.37	3.19
225	CDF Run-1 electron A_{ch}, $p_{T\ell} > 25$ GeV	11	8.9	0.81	-0.32
227	CDF Run-2 electron A_{ch}, $p_{T\ell} > 25$ GeV	11	14	1.24	0.67
234	DØ Run-2 muon A_{ch}, $p_{T\ell} > 20$ GeV	9	8.3	0.92	-0.02
240	LHCb 7 TeV 35 pb^{-1} W/Z $d\sigma/dy_\ell$	14	9.9	0.71	-0.73
241	LHCb 7 TeV 35 pb^{-1} A_{ch}, $p_{T\ell} > 20$ GeV	5	5.3	1.06	0.30
260	DØ Run-2 Z rapidity	28	17	0.59	-1.71
261	CDF Run-2 Z rapidity	29	48	1.64	2.13
266	CMS 7 TeV 4.7 fb^{-1}, muon A_{ch}, $p_{T\ell} > 35$ GeV	11	12.1	1.10	0.37
267	CMS 7 TeV 840 pb^{-1}, elec. A_{ch}, $p_{T\ell} > 35$ GeV	11	10.1	0.92	-0.06
268	ATLAS 7 TeV 35 pb^{-1} W/Z cross sec., A_{ch}	41	51	1.25	1.11
281	DØ Run-2 9.7 fb^{-1} elec. A_{ch}, $p_{T\ell} > 25$ GeV	13	35	2.67	3.11
504	CDF Run-2 inclusive jet production	72	105	1.45	2.45
514	DØ Run-2 inclusive jet production	110	120	1.09	0.67
535	ATLAS 7 TeV 35 pb^{-1} incl. jet production	90	50	0.55	-3.59
538	CMS 7 TeV 5 fb^{-1} incl. jet production	133	177	1.33	2.51

Aspects of the CT14 analysis

- PDFs are parametrized at init scale $Q_0 = 1.3$ GeV.
low-Q
- large-x data not included to avoid large non-perturbative contributions ($W > 3.5$ GeV)
- more flexible parametrizations for gluon, d/u at large x, both d/u and $\bar{d}/\bar{u}$ at small x, and strange ($\bar{s} = s$) PDFs.
- Non-perturbative parametrization employing Bernstein polynomials $P_a(x)$: $xf_a(x) = x^{a_1}(1-x)^{a_2}P_a(x)$

  This reduces the correlation among its coefficients.
- CT14: 28 shape parameters, while CT10 has 25.
- S-ACOT-χ NNLO for the heavy flavor treatment
- NNLO calculations for *DIS*, *DY*, *W*, *Z* cross sections, for the jet cross sections and DIS charged currents we only use the NLO calculation but with NNLO PDF.

Aspects of the CT14 analysis: $\alpha_s(M_Z)$

- central value of $\alpha_s(M_Z) = 0.118$ has been assumed in the global fits at NLO and NNLO, but
- PDF sets at alternative values of $\alpha_s(M_Z)$ are provided.
- CT14 prefers $\alpha_s(M_Z) = 0.115^{+0.006}_{-0.004}$ at NNLO (0.117 ± 0.005 at NLO) at 90 % confidence level (C.L.).

Uncertainties from the global QCD fits are larger than those of the data from LEP and other experiments included into the world average *Chin.Phys.C* (2014).

CT14 $\alpha_s(M_Z)$ central is consistent with the world average value.

CT14: DGLAP evolution

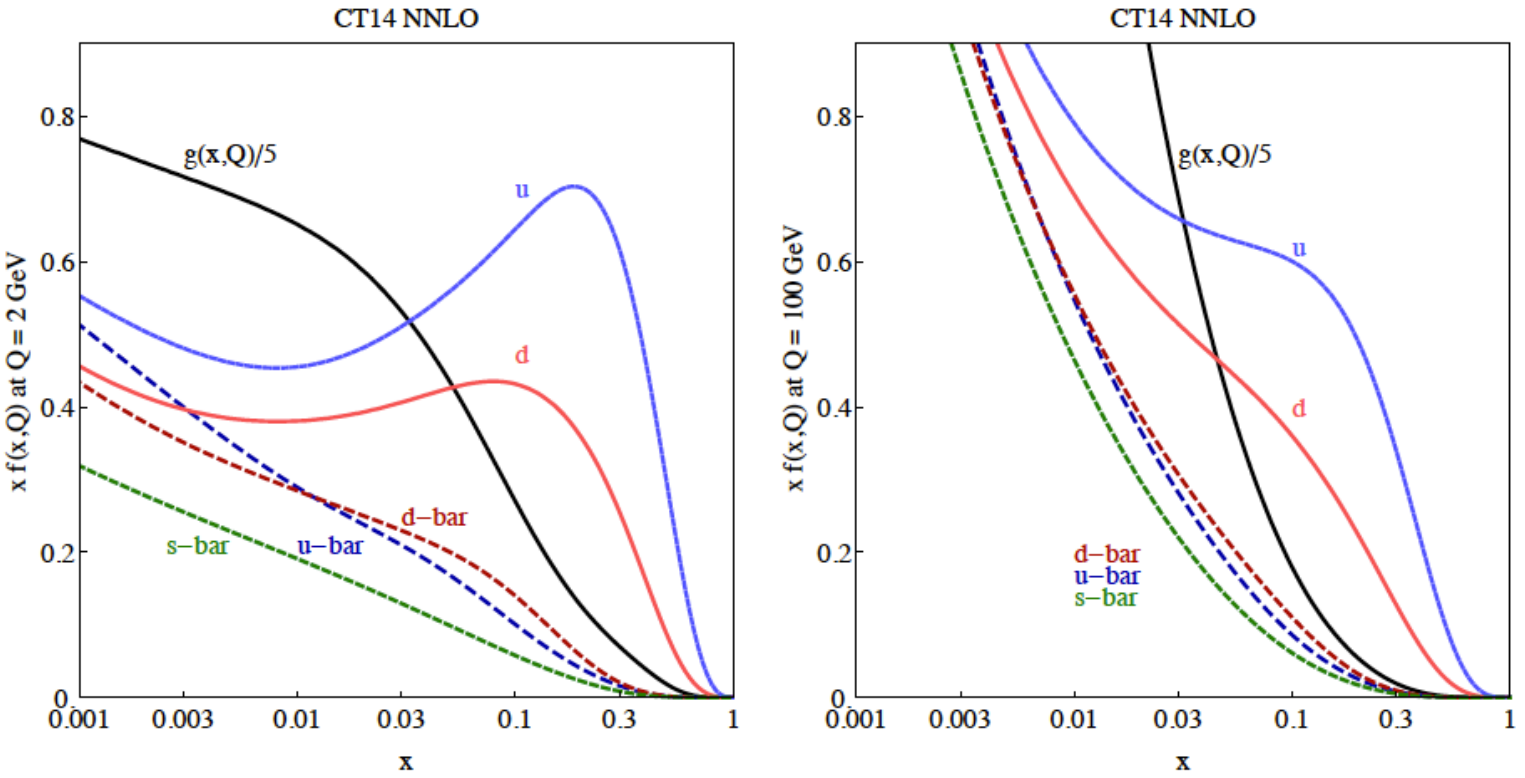

The CT14 PDFs $u, \overline{u}, d, \overline{d}, s = \overline{s}$, and g, evolved up to $Q = 2$ GeV and $Q = 100$ GeV.

IMPACT OF LHC RUN I measurements on the PDFs

CT14 vs CT10 at NNLO 90% C.L.

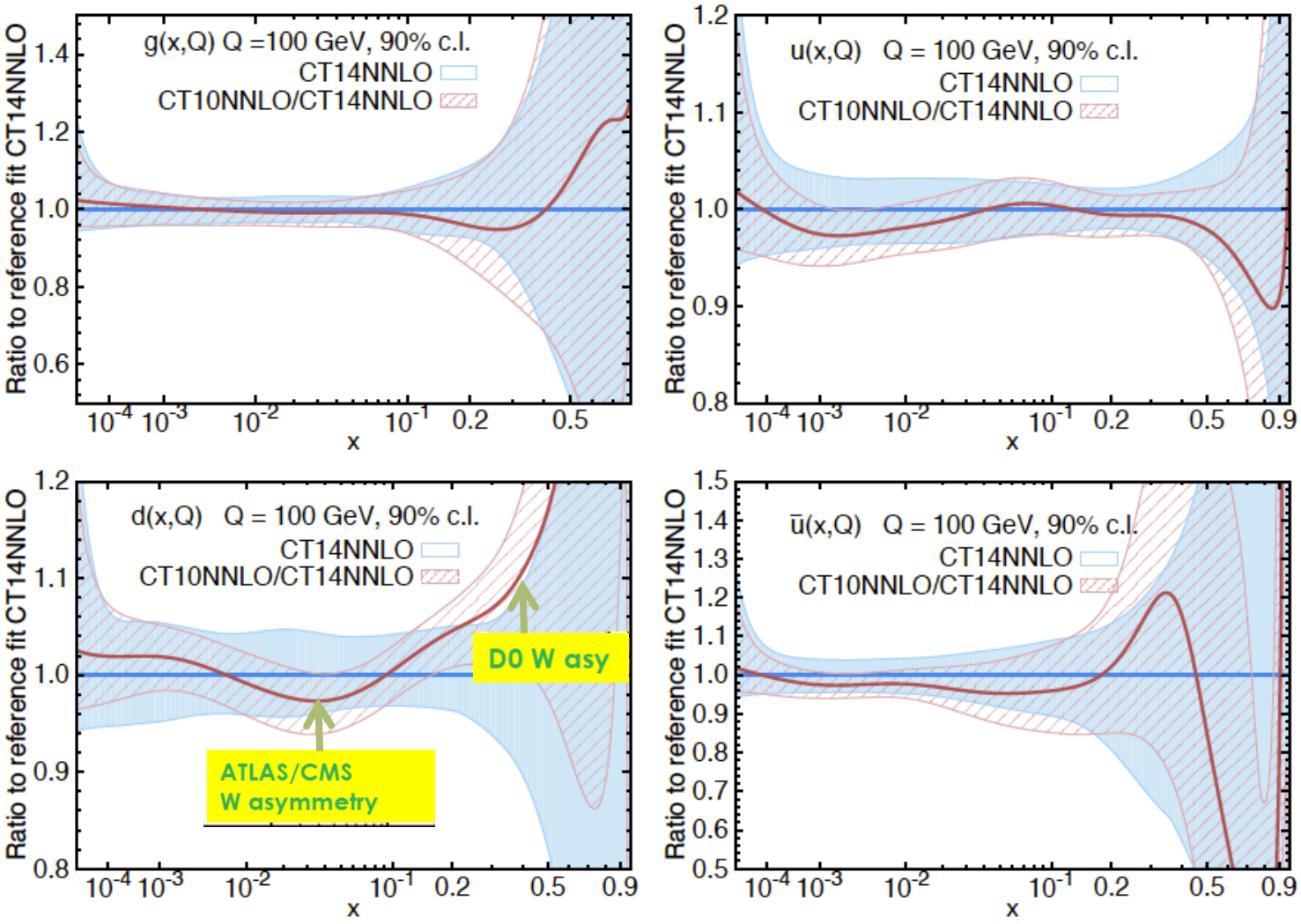

- ATLAS, CMS 7 TeV W/Z prod. $\Rightarrow$ d-quark increased by 5% at $x \approx 0.05$.
- D0 ele charge asy data $\Rightarrow$ d highly reduced at $x \geq 0.1$ and u moderately increased.

CT14 $d(x,Q)/u(x,Q)$ ratios

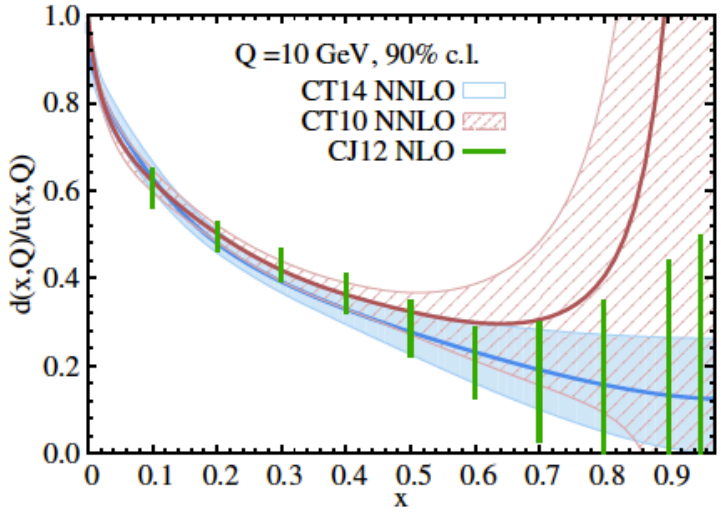

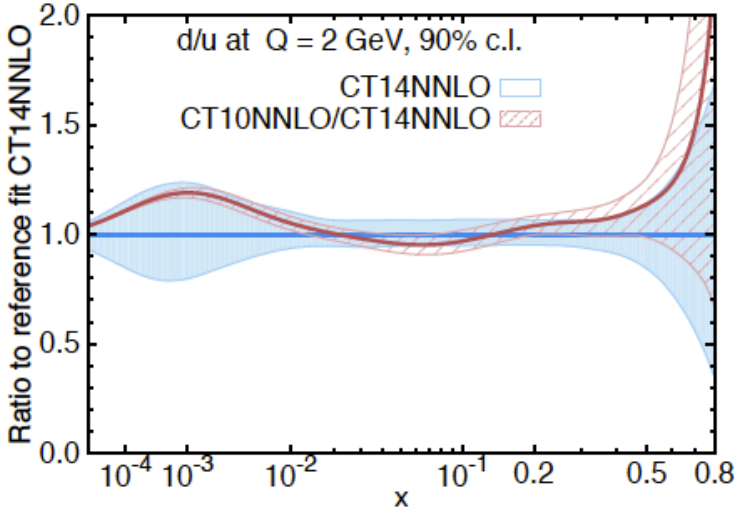

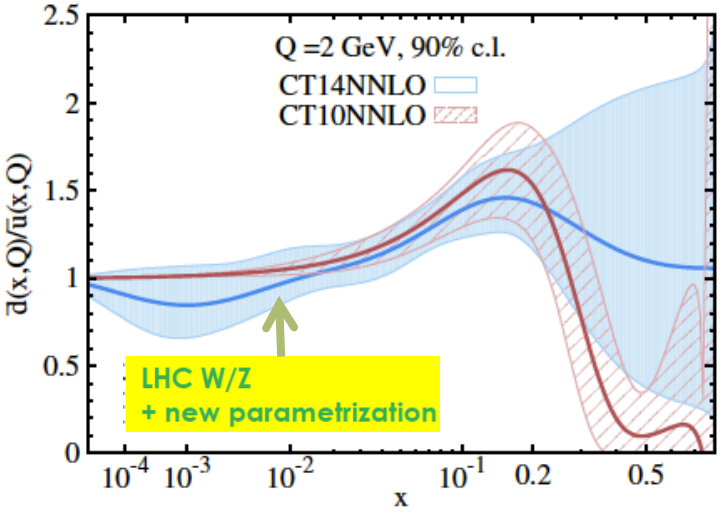

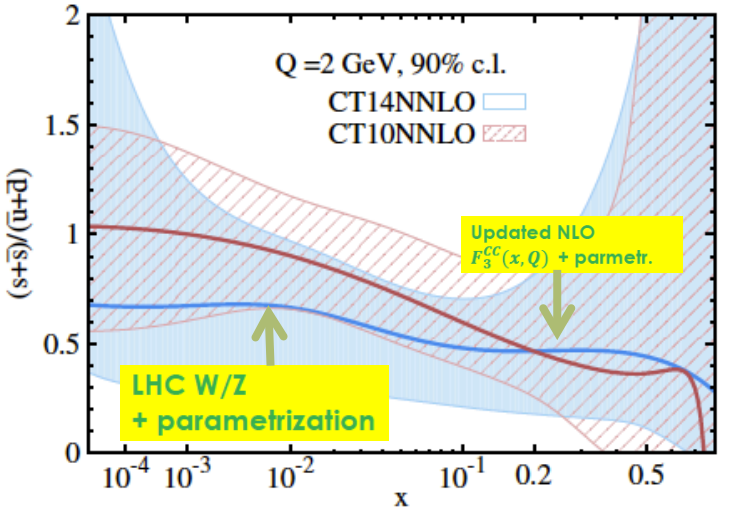

- 9.7 fb^{-1} D0 charge asy $\Rightarrow$ reduction of the central ratio at $x > 0.1$,
- new parametrization form $\Rightarrow$ increased uncertainty at $x < 0.05$
- s reduction at $x > 0.01$ $\Rightarrow$ smaller ratio $(s+\bar{s})/(\bar{u}+\bar{d})$. The $SU(3)$-symmetric asymptotic solution at $x \to 0$ is still allowed in CT14: bigger unc. $x \approx 10^{-5}$.

Let's explore the impact of new data sets

In 2015, the H1 and ZEUS collaborations released a novel combination of measurements of inclusive DIS cross sections at HERA: the HERA2 combined measurements:
The H1 and ZEUS Collaboration, EPJC75 (2015) 580, arXiv:1506.06042.

The HERA2 data exhibit a significantly reduced systematic uncertainty.

We explored the impact of these data on the CT14 analysis

CTEQ-TEA PDFs and HERA run I+II Combined Data

Tie-Jiun Hou,[1,*] Sayipjamal Dulat,[2,3,4,†] Jun Gao,[5,‡] Marco Guzzi,[6,§] Joey Huston,[4,¶]
Pavel Nadolsky,[1,**] Jon Pumplin,[4,††] Carl Schmidt,[4,‡‡] Daniel Stump,[4,§§] and C.–P. Yuan[4,¶¶]

CT14HERA2: arXiv:1609.07968 [hep-ph], to appear on PRD (2017)

The HERA run I+II (=HERA2) measurements

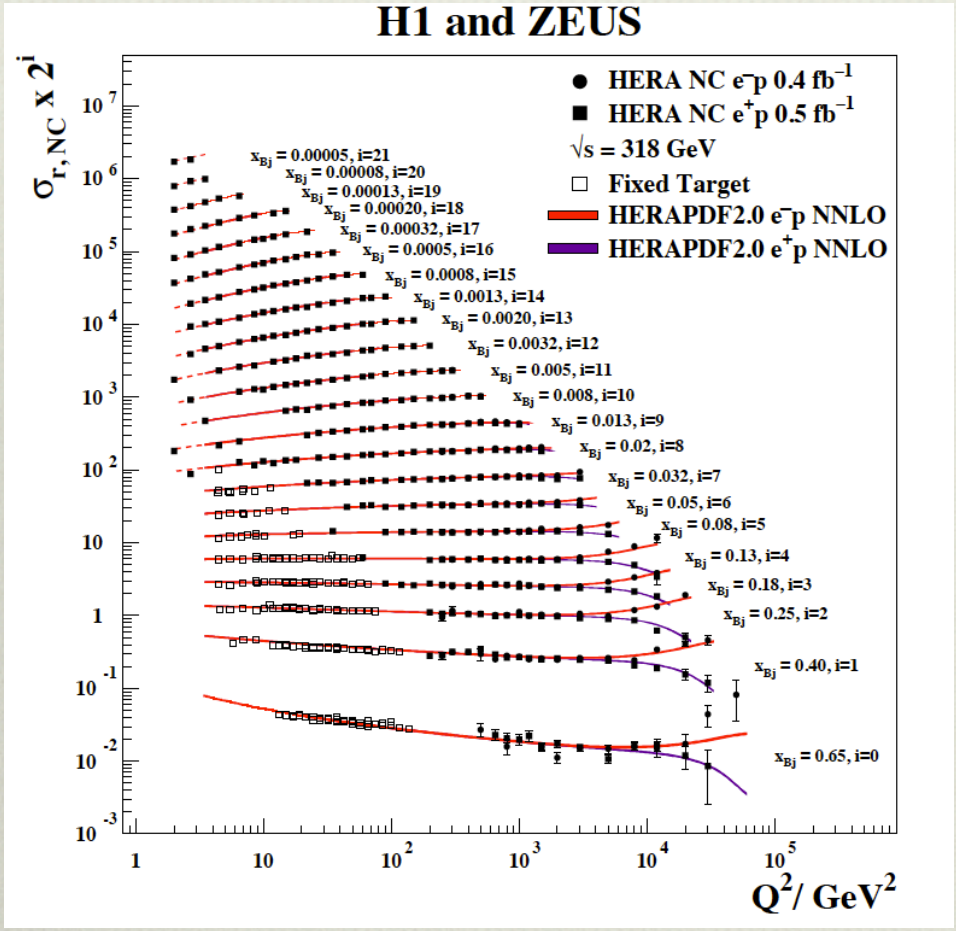

H1 and ZEUS combination of DIS cross sections for NC and CC
H1 and ZEUS Coll. 1506.06042 EPJ2015

Back bone measurements for PDF determination

Neutral Current		Charged Current
e-p	[Ep=920 GeV]	[Ep=920 GeV]
e+p	[Ep=920 GeV]	[Ep=920 GeV]
e+p	[Ep=460 GeV]	
e+p	[Ep=575 GeV]	
e+p	[Ep=820 GeV]	

CT14HERA2 ⇒ The CTEQ-TEA PDFs have been refitted NLO and NNLO by using the global CT14 data ensemble, but with the HERA2 measurements in place of HERA1.

Other changes w.r.t. CT14

CT14HERA2 global fit 3287 data points in total compared to 2947 in the original CT14:

1) The NMC muon-proton inclusive DIS data on F2p are dropped (cannot be fitted well; data is influenced by some unknown or underestimated systematic errors). We continue to include the NMC proton to deuteron ratio data on F2p /F2d.

2) The data table for the CMS 7 TeV 5 fb-1 inclusive jet experiment has been updated: no appreciable effects on the PDFs.

3) Introduction of 1 free parameter in the s(x,Q0) parametrization (Q0=1.3 GeV), in the end the number of eigenvector sets is 56 as in CT14.

$\chi^2_{\mathrm{CT14_{HERA2},NNLO}}/N_{pts} = 3596/3287 = 1.09$ $\chi^2_{\mathrm{CT14,NNLO}}/N_{pts} = 3250/2947 = 1.10$

Impact of HERA2 data on the PDFs compared to the CT14 fit

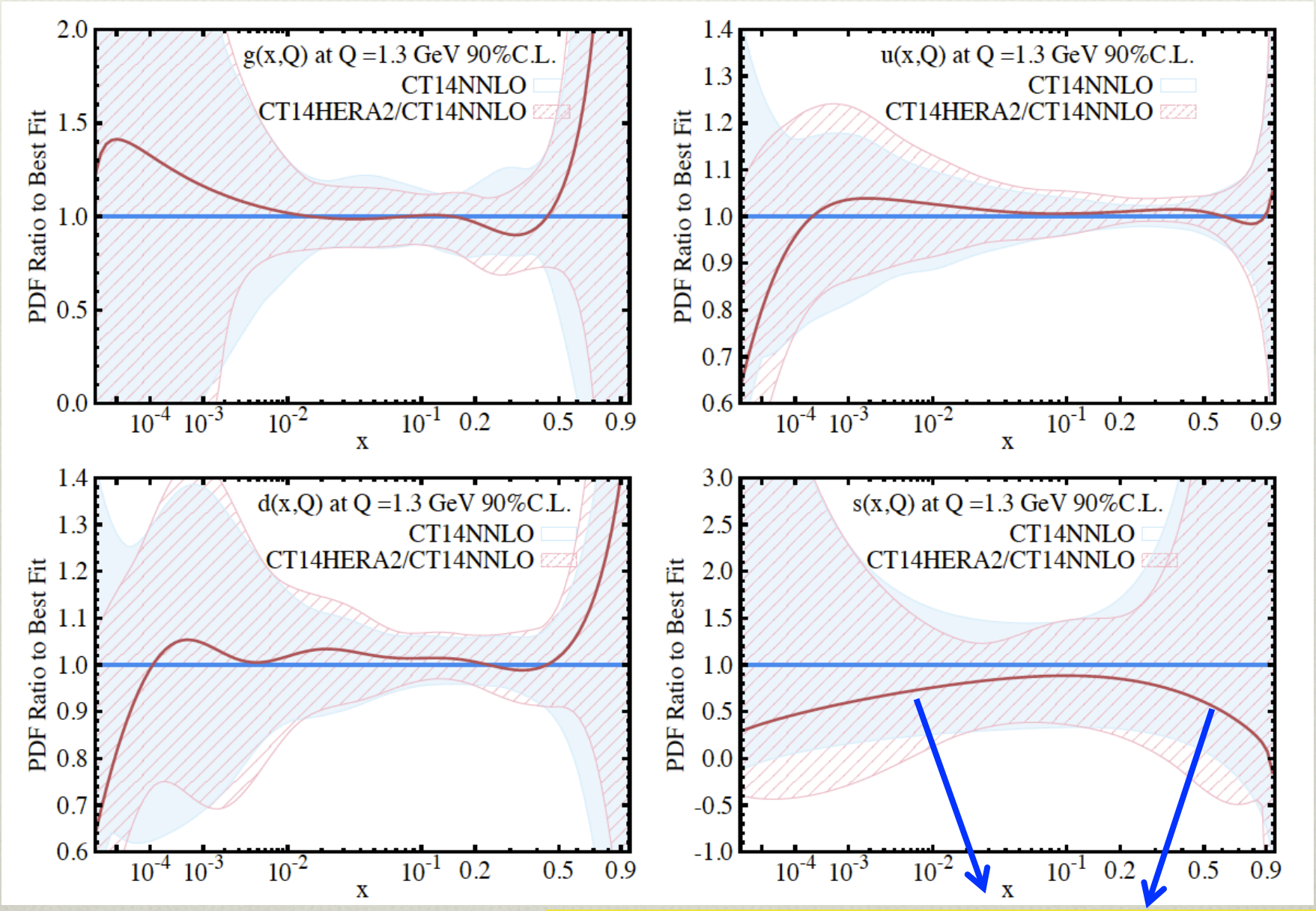

HERA2: changes in g, u, d

s(x,Q) reduction mainly due to more flexible param

Impact of HERA2 data on the PDFs compared to the CT14 fit

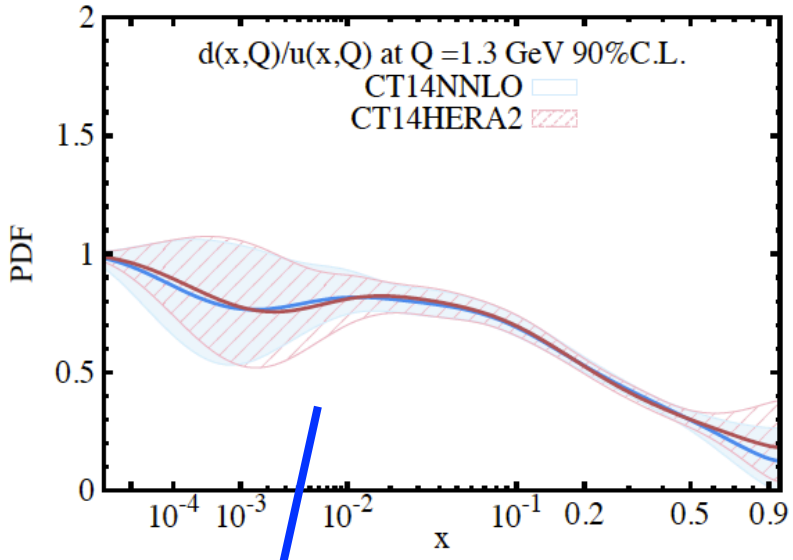

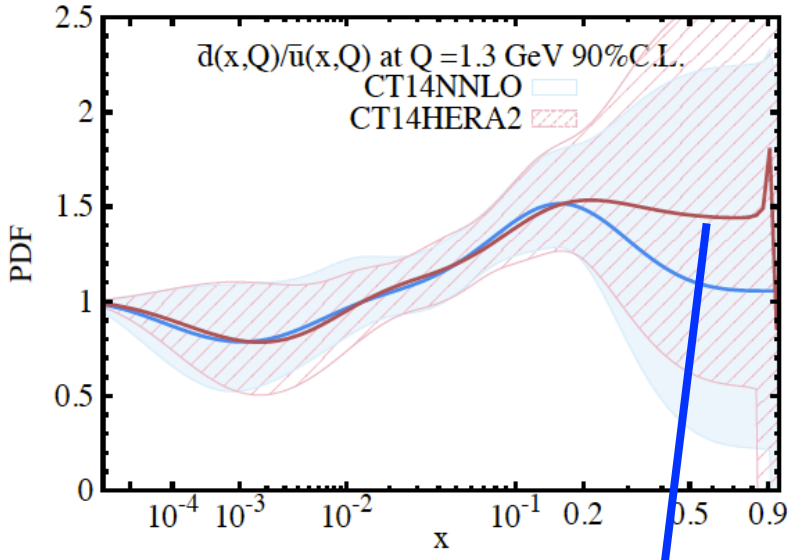

d/u almost unchanged

db/ub>1: s(x,Q) more flexible param.

s(x,Q) more flexible param.

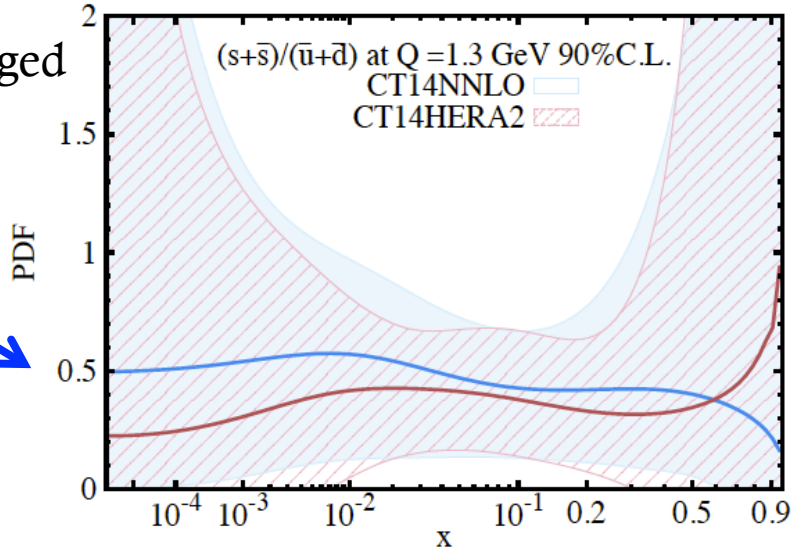

red line=CT14HERA2 NNLO; blue line=CT14NNLO

Consistency of the HERA1 and HERA2 data with the other data sets (*non*-HERA)

	$\chi^2_{\rm HERA1}$ (wt); $N_{\rm pts} = 579$	$\chi^2_{\rm HERA2}$ (wt); $N_{\rm pts} = 1120$
CT14(NLO)	590	1398
NLO10	576 (1.0)	1404 (0.0)
NLO55	586 (0.5)	1374 (0.5)
$\rm CT14_{HERA2(NLO)}$	595 (0.0)	1373 (1.0)
CT14(NNLO)	591	1469
NNLO10	583 (1.0)	1458 (0.0)
NNLO55	596 (0.5)	1411 (0.5)
$\rm CT14_{HERA2(NNLO)}$	610 (0.0)	1402 (1.0)

*) CT14 NLO and NNLO: no refitting.
*) NLO10(NNLO10), NLO55(NNLO55), CT14HERA2NLO(NNLO) are made with weights {1, 0}, {0.5, 0.5} or {0, 1} for the HERA1 and HERA2 data sets, respectively. (The {1, 0} fits are not identical to CT14 because they were made (i) with a slightly more flexible parametrization for the strange quark PDF, (ii) without the NMC F2p measurements, and (iii) with an updated data table for CMS jet production.)
*) chi^2 for the *non*-HERA is essentially unchanged as we vary the balance of HERA1 and HERA2 data

Overall goodness of the CT14HERA2 fit

CT14HERA2 NLO χ^2/N_{pts} = 1.07

CT14HERA2 NNLO χ^2/N_{pts} = 1.09

For the HERA2 data after refitting we find

χ^2_{HERA2}/N_{pts} = 1.22 at NLO

χ^2_{HERA2}/N_{pts} = 1.25 at NNLO

The NLO fit has a lower value of global 2 than the NNLO fit. This is a robust result: it is independent of whether HERA1 or HERA2 data set is used. It is also still true if $\alpha_s(M_Z)$, m_b, and m_c are varied as free parameters—separately, of course, for NLO and NNLO. The conclusions still hold if the kinematic cut Q_{cut} is raised.

We find larger values w.r.t. HERA1 (which gives approx 1.02) at both NLO and NNLO

Is it from a few isolated data points, or from a systematic difference between data and theory?

…elevated values of chi2 for HERA2 do not arise from a single (x,Q) kinematic region.

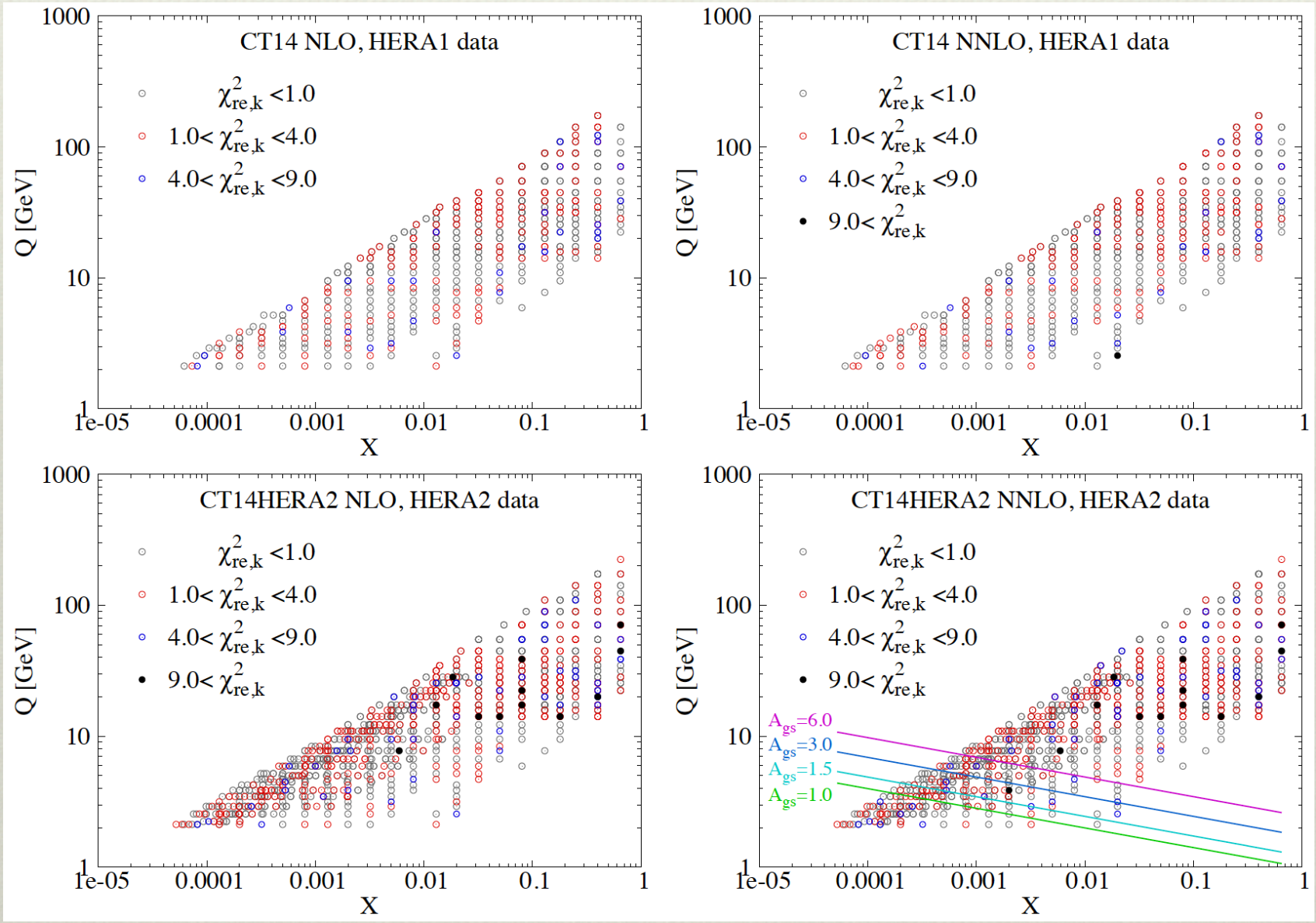

Distribution of reduced-chi2,k of HERA1 and HERA2 ensembles in the (x,Q) plane, for the CT14 (upper row) and CT14HERA2 (lower row) fits, respectively.

Varied statistical weights for the HERA2 data

An interesting way to assess the impact of the HERA2 combined data is to vary the weight given to this data set in the global chi^2 function.

CT14HERA2: varied statistical weights for the HERA2 data

Impact on the chi^2/Npts:

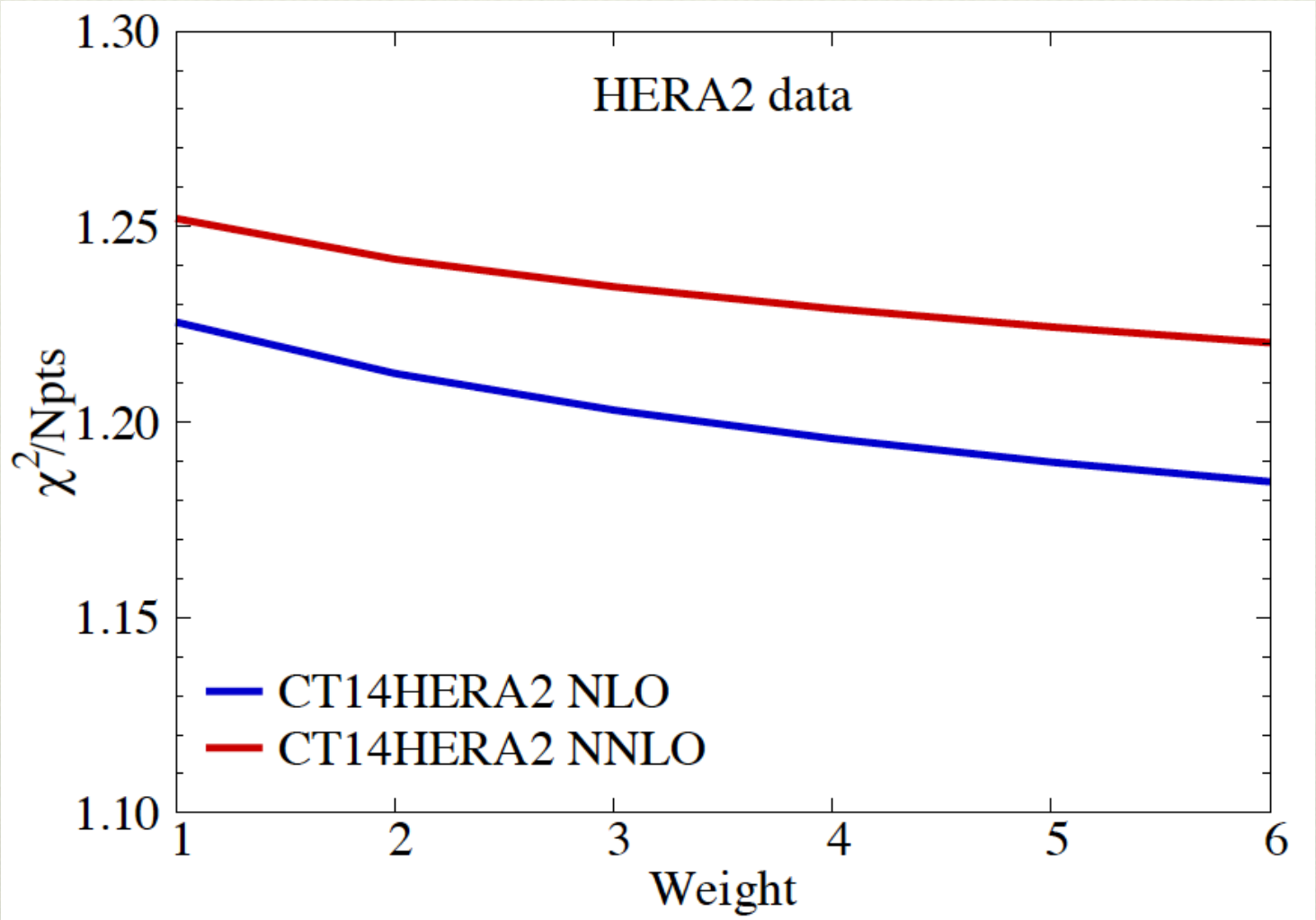

Increasing the weight of the HERA2 data must cause chi^2/Npts to decrease for that data. But the change of chi^2 is not large—only about − 5% for a factor of 6 extra weighting.

CT14HERA2: varied statistical weights for the HERA2 data

Impact on the PDFs:

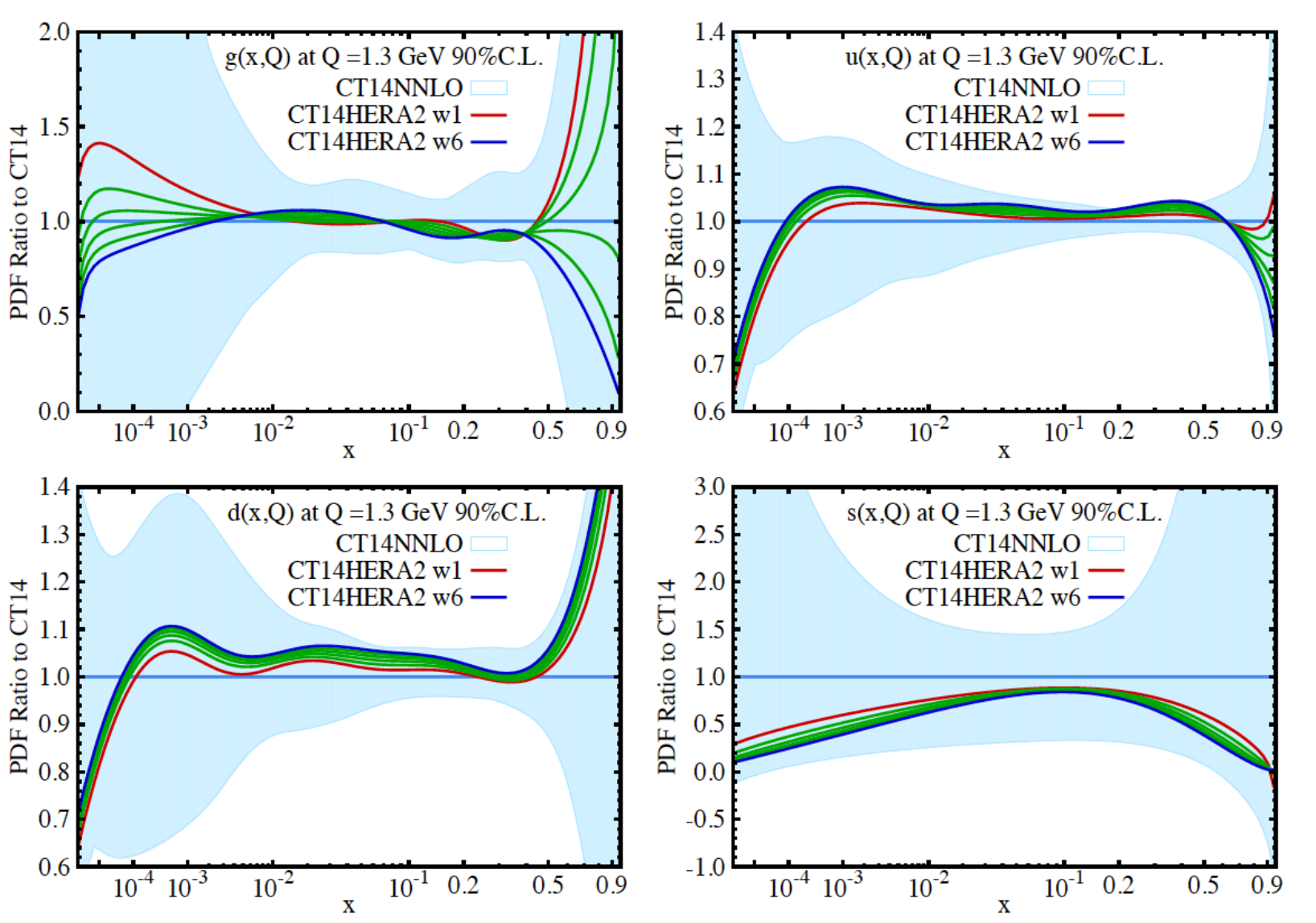

Comparison of CT14HERA2 PDFs at Q = 1.3 GeV within the CT14(NNLO) uncertainty band. Each curve represents the ratio of CT14HERA2/CT14 for a particular value of the weight assigned to the HERA2 data in the fit. The weight factors vary from 1 to 6.

IMPACT OF DATA SELECTION CUTS ON THE FIT TO HERA2 DATA

CT14HERA2: impact of data selection cuts on the fit

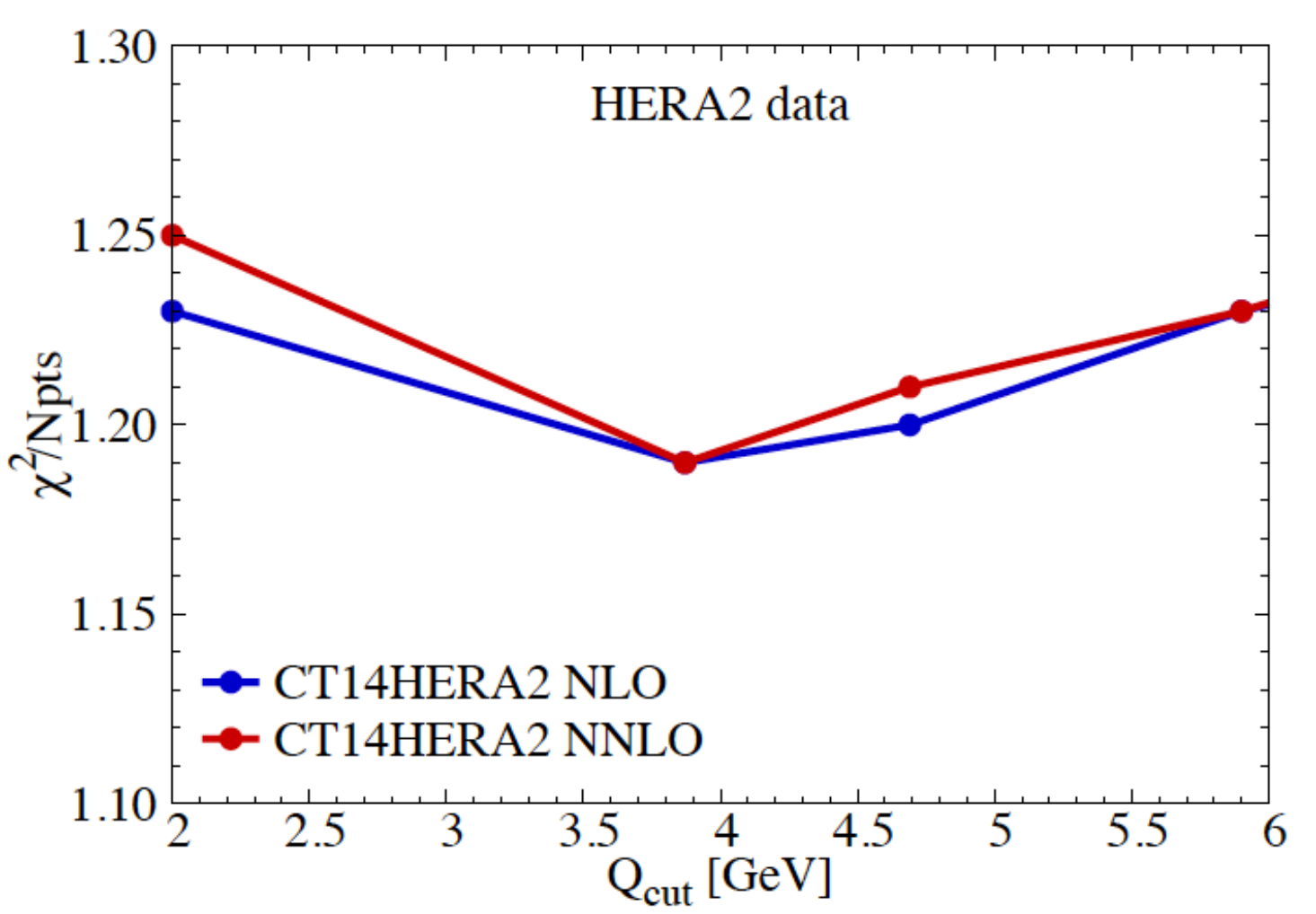

chi^2/Npts for the HERA2 data (all 4 subprocesses) as a function of Qcut. When the low-Q data points are discarded by the cut, the systematic errors become less important: the chi^2 nuisance term in the global chi^2 definition reduces. The overall net change in chi^2/Npts is mild.

Dependence on the geometric rescaling variable

$$A_{\rm gs} = x^{\lambda} Q^2$$

where λ = 0.3, (Stasto, Golec-Biernat, Kwiecinski PRL 2001,
Caola, Forte, Rojo PLB 2010,
CT10 analysis PRD 2010)

Ags has been used in previous analyses to search for possible deviations from DGLAP evolution due to saturation or small-x related phenomena.

The basic method can be briefly described as follows:

(i) generate PDFs using data in the kinematic region above the Ags cut in the x and Q plane, where the NLO/NNLO DGLAP factorization is supposed to be valid;
(ii) use DGLAP evolution equations to evolve these PDFs down to the low x and Q region below the Ags cut, where one might expect possible deviations;
(iii) compare predictions to the data in the low Ags region, which was not used for PDF determination

CT14HERA2: impact of data selection cuts on the fit

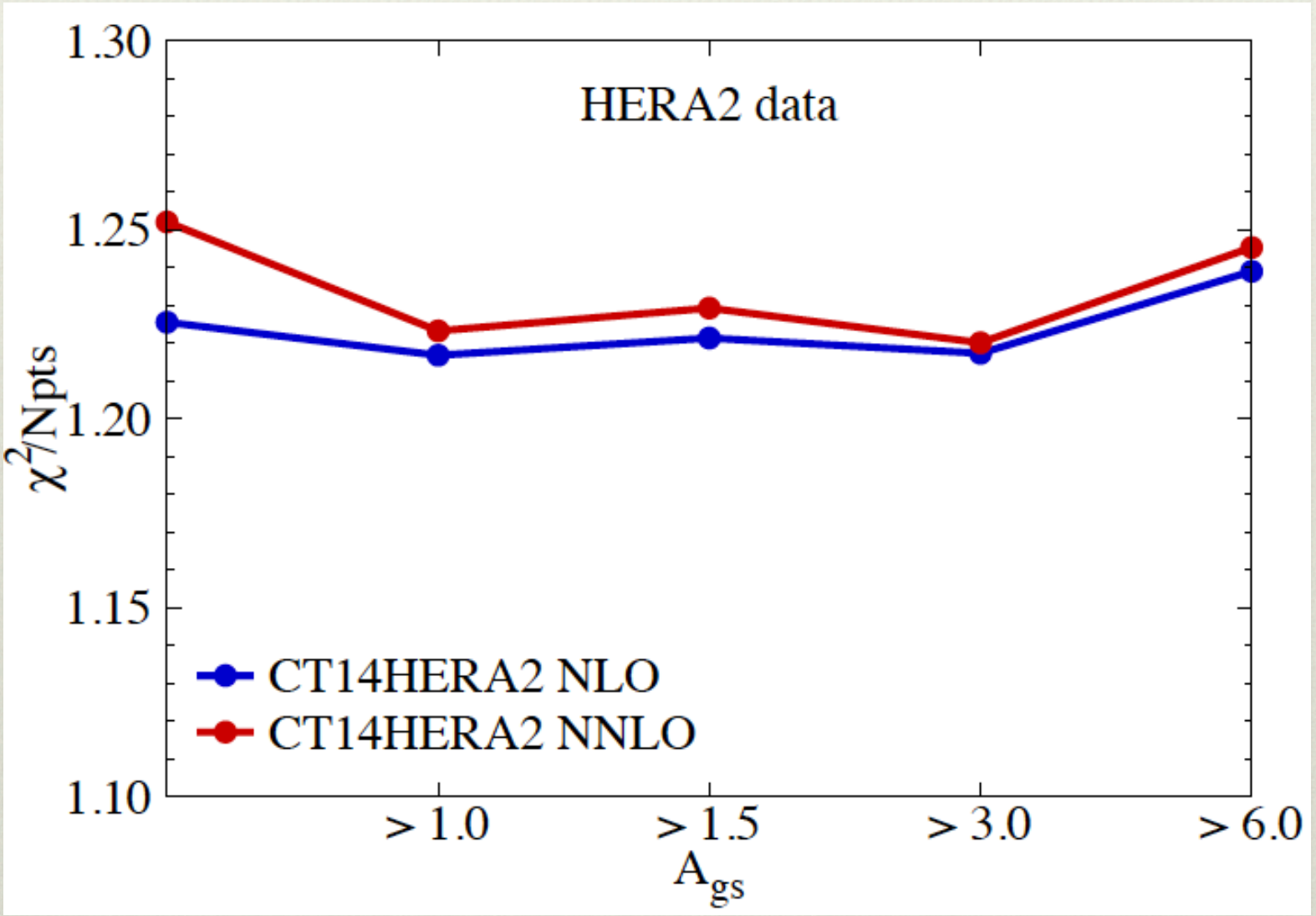

chi^2/Npts for the HERA2 data and CT14HERA2PDFs as a function of the geometric scaling variable Ags

We have also studied a more flexible gluon PDF by introducing one more nonperturbative shape parameter, in the fit.

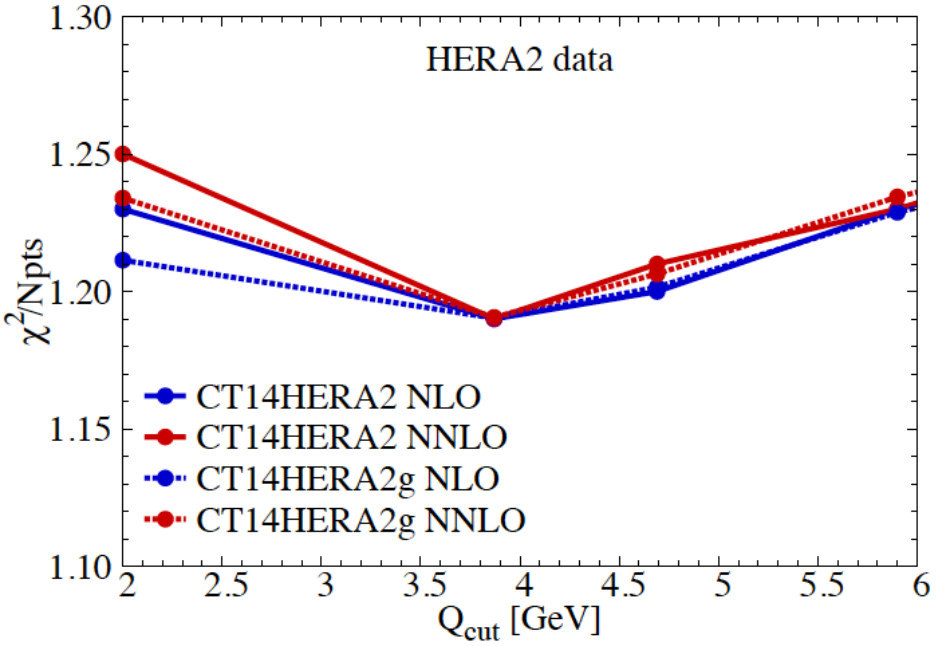

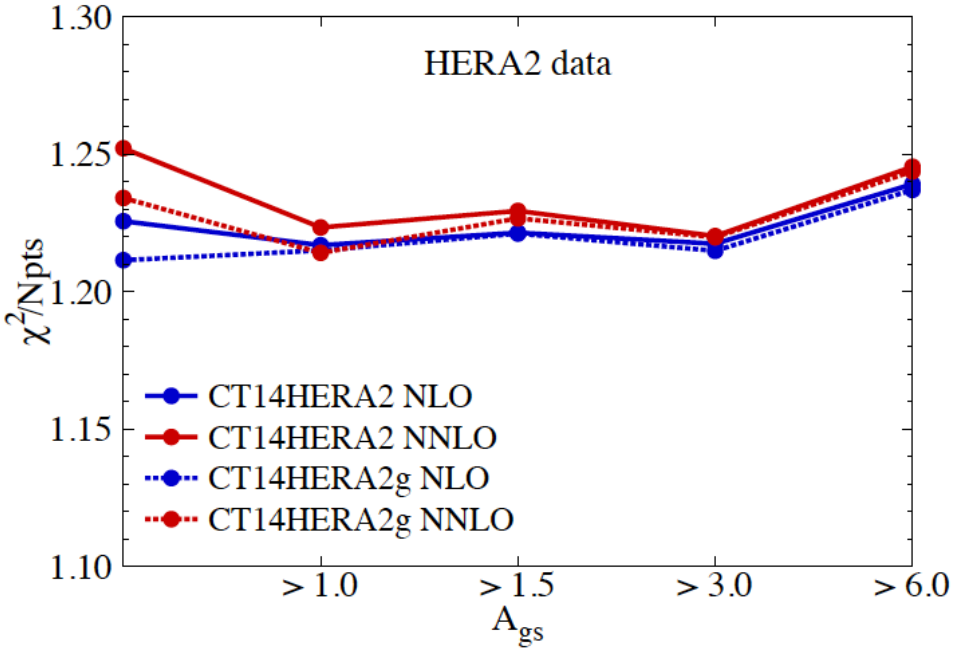

Even including the data points below the Ags cut (though still with Q > 2 GeV) in the calculation of chi^2 in the final comparison while fitting only the data above the Ags cut we find similar conclusions obtained in the CT10 study (2010): the spread of the outcomes appears to be too wide to corroborate the existence of the deviations from DGLAP.

Observations:

i) When eliminating points at the lowest Q or Ags from the fit, we observed an increase in the PDF uncertainty at these points.

ii) we observe some growth by comparable amounts in both the chi^2 for the excluded points and its PDF uncertainty.

iii) In separate fits with a more flexible gluon parametrization, we also find that the value of chi^2/Npts for the NLO fit is larger than the NNLO fit by about 0.1 unit, which is about the same size as the variation from including the Ags > 1.5 cut in the fit.

The parameterization dependence of chi^2 in the fit with the Ags cut is comparable to the increase in chi^2 (same features found in the CT10 study PRD 2010)

We conclude that our analysis of the HERA2 data does not indicate clear deviations from DGLAP evolution.

In two recent PDF analyses performed at NLO in QCD:

PROSA EPJC (2015); Gauld, Rojo (2016);

it has been observed that differential cross section measurements for heavy-flavour production of the LHCb collaboration at the LHC probe the very forward range of the heavy-hadron rapidity and are sensitive to the gluon PDF at low x.

In particular, they can probe the gluon and sea-quark distributions at partonic fraction x approx 10^-6 and set tighter constrains on the gluon parametrization in that x-range.

Future global PDF analyses will benefit from the constraints imposed by such measurements, in particular in fits testing DGLAP evolution with variable cuts imposed on the data.

Conclusions I

- **The differences between CT14HERA2 and CT14 PDFs are smaller than the uncertainties of the PDFs, as estimated by the Hessian method of error propagation.**

- **The standard CT14 PDFs should continue to be used for making predictions to compare against current and future LHC data.**

- **CT14HERA2 PDFs available in the LHAPDF format for specialized studies, such as those that are sensitive to behavior of strange (anti)quark PDFs.**

Conclusions II

- LHC unprecedented energies brought us in a new precision era.

- Massive efforts are going on to constrain proton structure:
PDF uncertainties still remain a limiting factor for precision at the LHC.

- Future looks promising & challenging at the same time:
Efforts in selecting new, highly sensitive measurements for constraining PDFs
-ttbar differential cross sections;
-inclusive jet production;
-Z+jet
-….

- Efforts on the theory side to make the most out of the recent NNLO calculations:
Fast implementations are mandatory for PDF determination in global analyses.

- High precision data ⇒ control on subleading effects (NLO EM corrections, photon PDFs, off-shell resonant production…) and theoretical uncertainties (scale dependence, heavy-quark schemes)

BACKUP

CT14 NNLO: agreement with data

Total of 2947 data points from 33 experiments
$\chi^2 = 3252$ at the best fit CT14 NNLO,
$\chi^2/N_{pt} = 1.10$.

Data and theory are in reasonable good agreement for most experiments
(next slides)

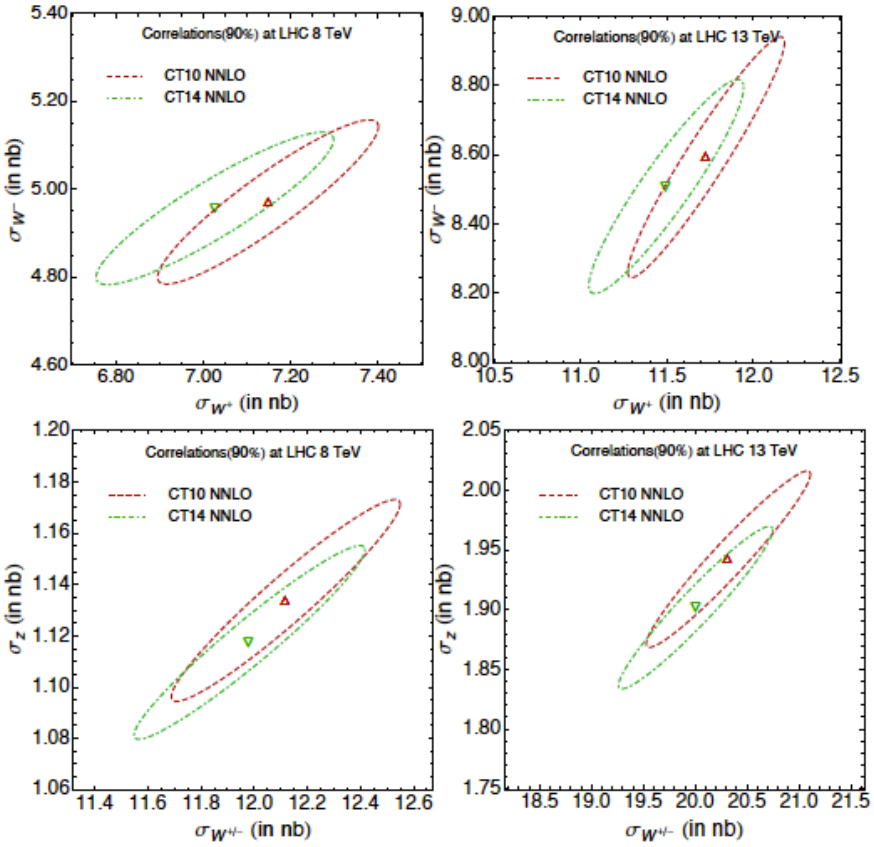

W/Z Correlations plots CT14 vs CT10 @ NNLO

CT14 NNLO: agreement with data

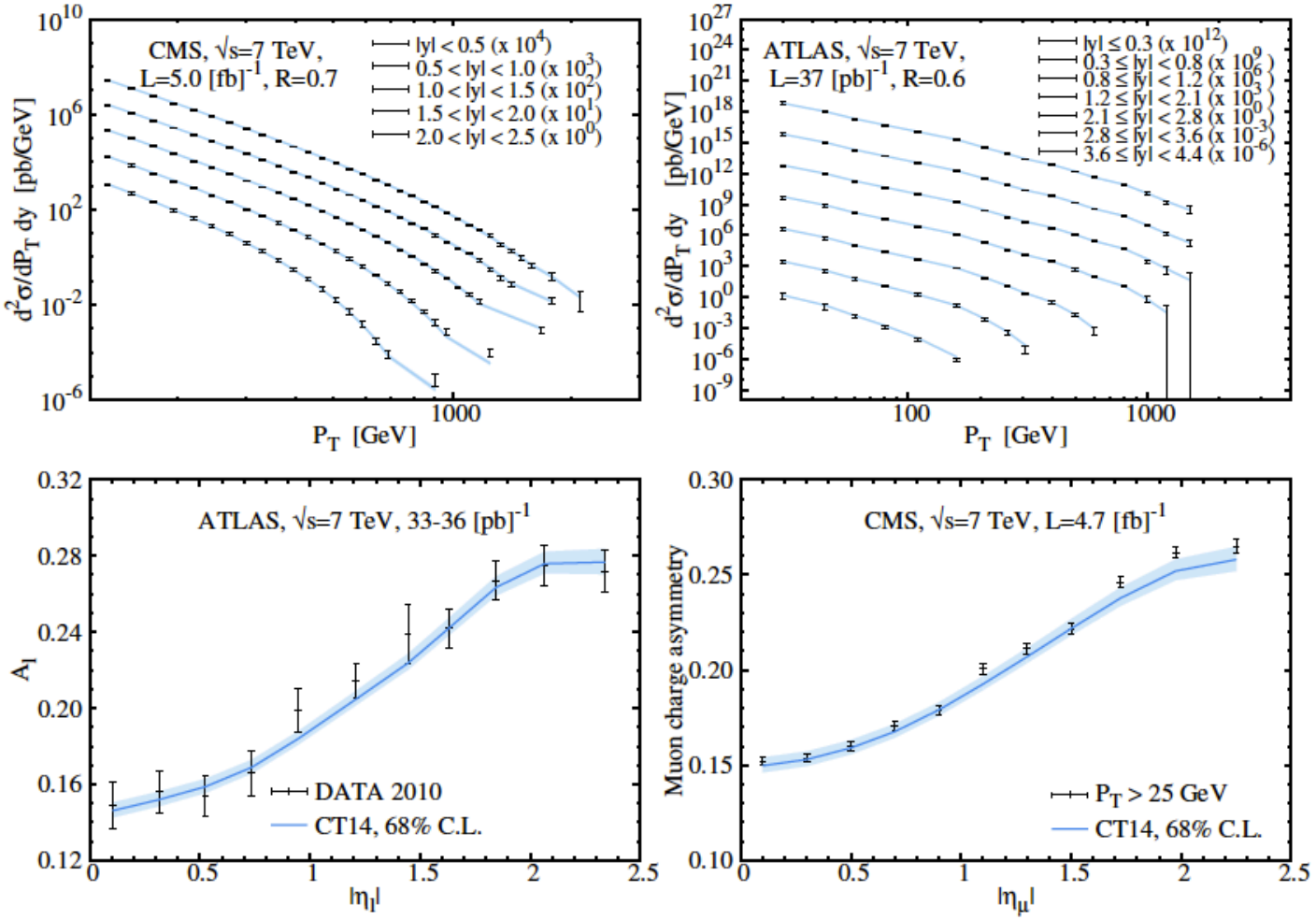

Inclusive jet production and W lepton charge asymmetry at the LHC 7 TeV

CT14 NNLO: agreement with data

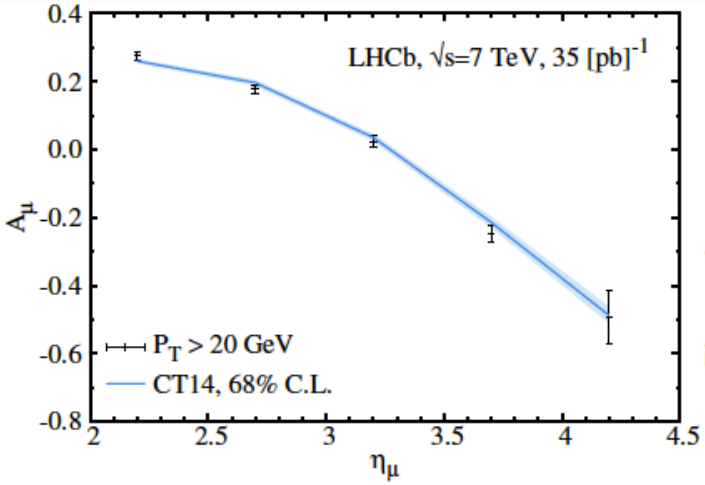

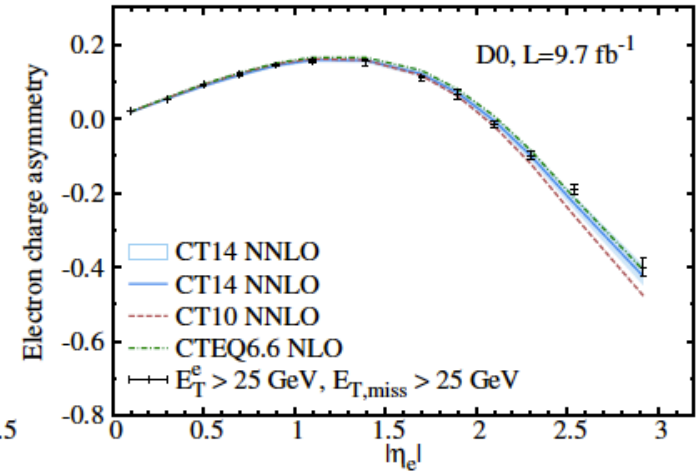

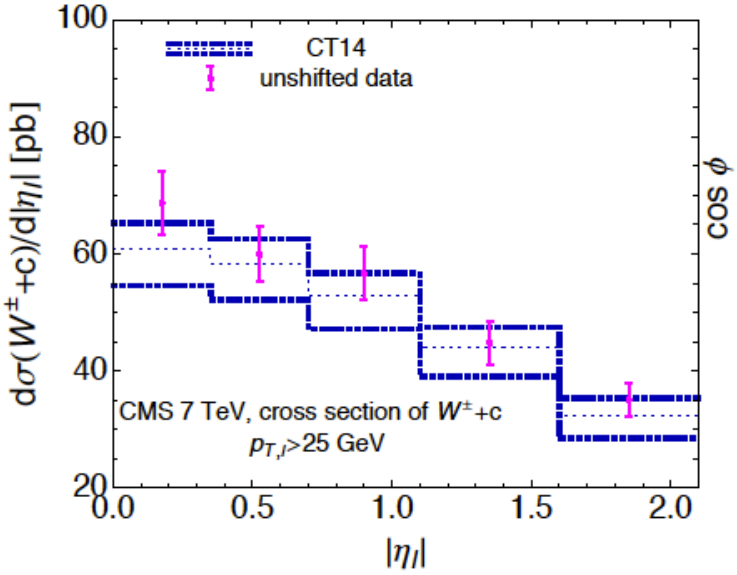

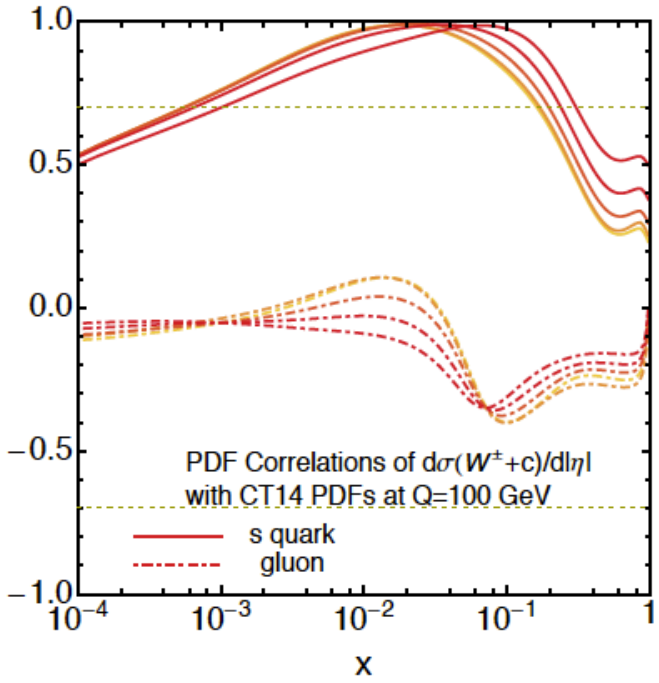

CT14 NNLO: agreement with data

Total inclusive $t\bar{t}$ cross section at NNLO in QCD with TOP++, (Czakon, Mitov, CPC 2014)

$pp \to t\bar{t}$ (pb), PDF unc., $\alpha_s = 0.118$	7 TeV	8 TeV	13 TeV
68% C.L. (Hessian)	$177 + 4.8\% - 3.9\%$	$250 + 3.9\% - 3.5\%$	$820 + 2.6\% - 2.7\%$
68% C.L. (LM)		$+4.8\% - 4.6\%$	$+2.9\% - 2.9\%$
$pp \to t\bar{t}$ (pb), PDF+α_s	7 TeV	8 TeV	13 TeV
68% C.L. (Hessian)	$+5.5\% - 4.6\%$	$+5.2\% - 4.4\%$	$+3.6\% - 3.5\%$
68% C.L. (LM)		$+5.1\% - 4.7\%$	$+3.6\% - 3.5\%$

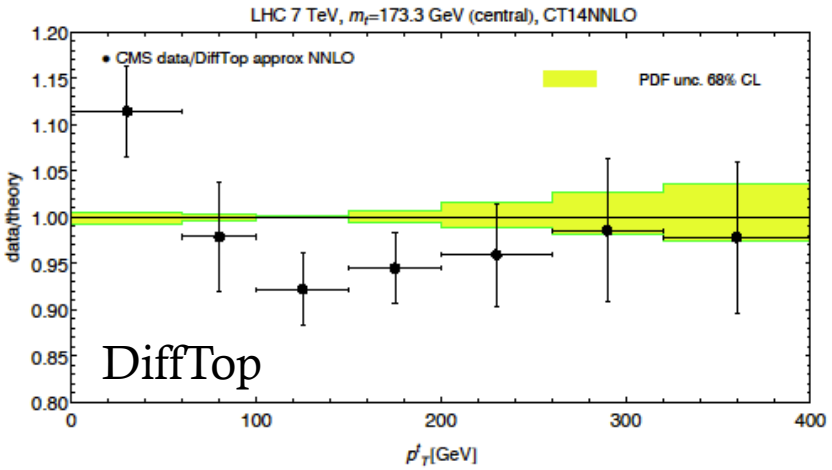

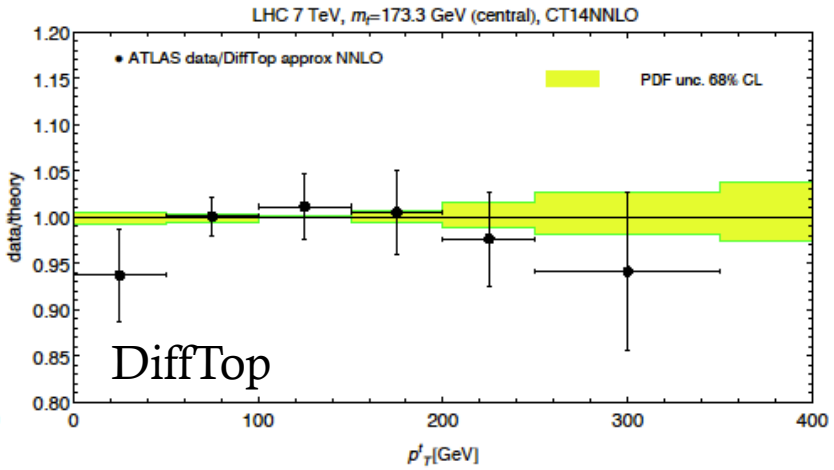

Approx NNLO p_T spectrum for the final state top-quark with DIFFTOP (M.G., Lipka, Moch, JHEP 2015)

CTEQ log-likelihood chi2 function: the reduced-chi2:

$$\chi^2_{\mathrm{re},k} = (D_k - T_k - \sum_\alpha \lambda_\alpha \beta_{k\alpha})^2 / s_k^2$$

$$s_k = \sqrt{s^2_{k,\mathrm{stat}} + s^2_{k,\mathrm{uncor\ sys}}}$$

$$\chi^2_{exp} = \sum_{k=1}^{N_{pts}} \chi^2_{\mathrm{re},k} + \sum_\alpha \lambda^2_\alpha \equiv \chi^2_{\mathrm{re}} + R^2$$

N = total number of points;
sk = total uncorrelated error on the measurement Dk, equal to the statistical and uncorrelated systematic errors on Dk added in quadrature.
$\beta_{k\alpha}$= correlation matrix
λ =nuisance parameter

Minimization of chi^2 with respect to the systematic parameters λ is realized algebraically

Goodness-of-fit characteristics for both HERA1 and HERA2 at NNLO

$Q_{\rm cut}$ [GeV]	no cut	2.00	3.87	4.69	5.90
$\chi^2/N_{pts}(N_{pts})$	(647)	1.02 (579)	0.93 (516)	0.93 (493)	0.91 (470)
$R^2/114(R^2)$		0.43(48.80)	0.24(27.34)	0.25(28.38)	0.25(28.48)
$\chi^2_{\rm re}/N_{pts}(N_{pts})$	(647)	0.94 (579)	0.89 (516)	0.87 (493)	0.84 (470)
NC e^+p	(434)	1.05 (366)	0.96 (303)	0.96 (280)	0.92 (257)
NC e^-p	(145)	0.74 (145)	0.75 (145)	0.75 (145)	0.75 (145)
CC e^+p	(34)	0.97 (34)	0.98 (34)	0.99 (34)	0.99 (34)
CC e^-p	(34)	0.53 (34)	0.53 (34)	0.53 (34)	0.53 (34)

CT14 - HERA1

$Q_{\rm cut}$ [GeV]	no cut	2.00	3.87	4.69	5.90
$\chi^2/N_{pts}(N_{pts})$	(1306)	1.25 (1120)	1.19 (967)	1.21 (882)	1.23 (842)
$R^2/170(R^2)$		0.51 (87.47)	0.29(49.11)	0.29 (48.99)	0.29 (49.40)
$\chi^2_{\rm re}/N_{pts}(N_{pts})$	(1306)	1.17 (1120)	1.14 (967)	1.15 (882)	1.18 (842)
NC e^+p	(1066)	1.11 (880)	1.06 (727)	1.06 (642)	1.09 (602)
NC e^-p	(159)	1.45 (159)	1.44 (159)	1.45 (159)	1.45 (159)
CC e^+p	(39)	1.10 (39)	1.10 (39)	1.10 (39)	1.10 (39)
CC e^-p	(42)	1.52 (42)	1.50 (42)	1.50 (42)	1.50 (42)

CT14HERA2 - HERA2

CT14HERA2: varied statistical weights for the HERA2 data

Impact on the PDFs:

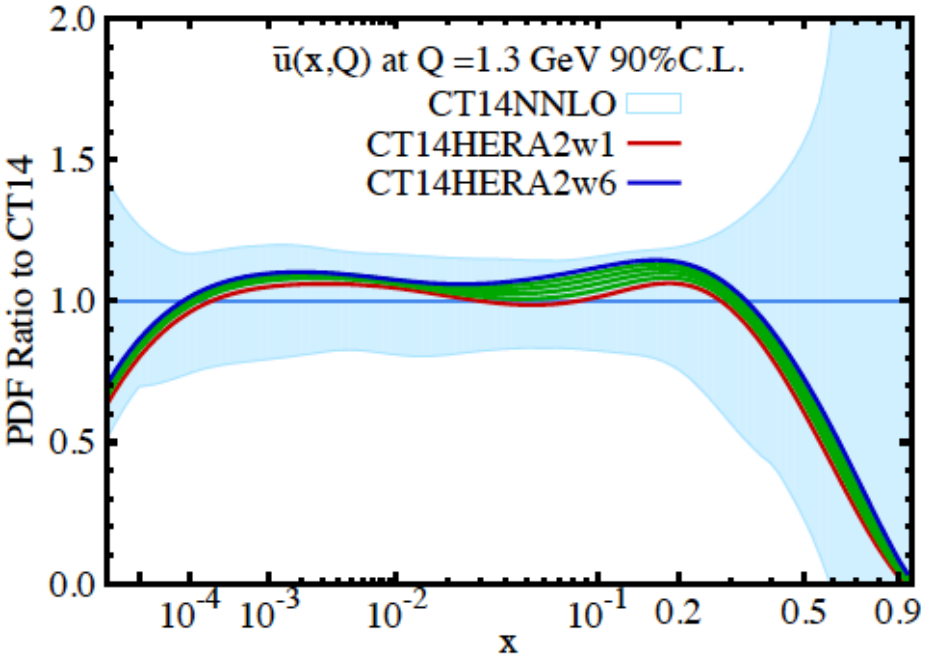

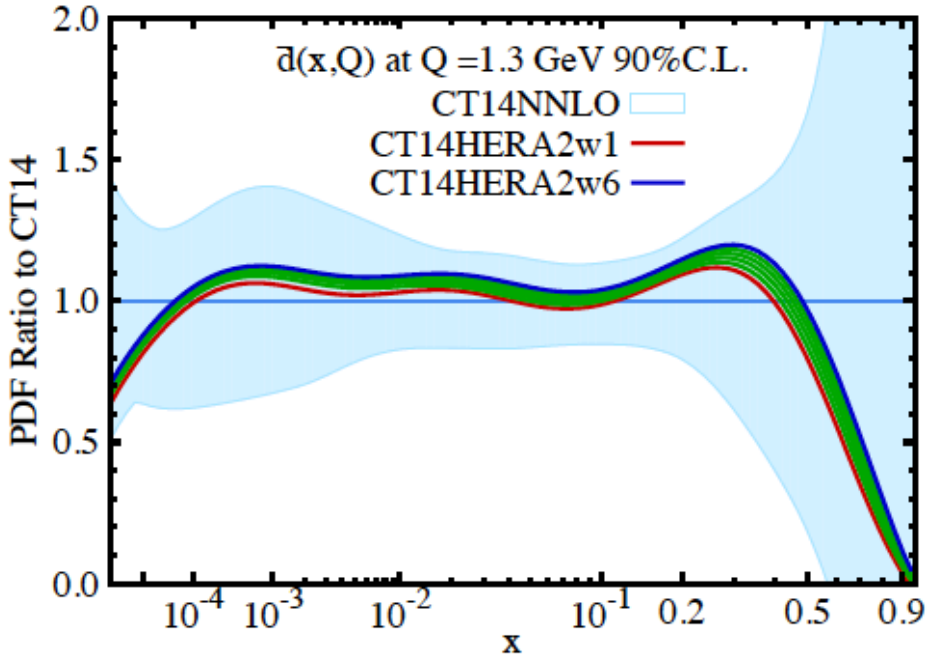

Comparison of CT14HERA2 PDFs at Q = 1.3 GeV within the CT14(NNLO) uncertainty band. Each curve represents the ratio of CT14HERA2/CT14 for a particular value of the weight assigned to the HERA2 data in the fit. The weight factors vary from 1 to 6.

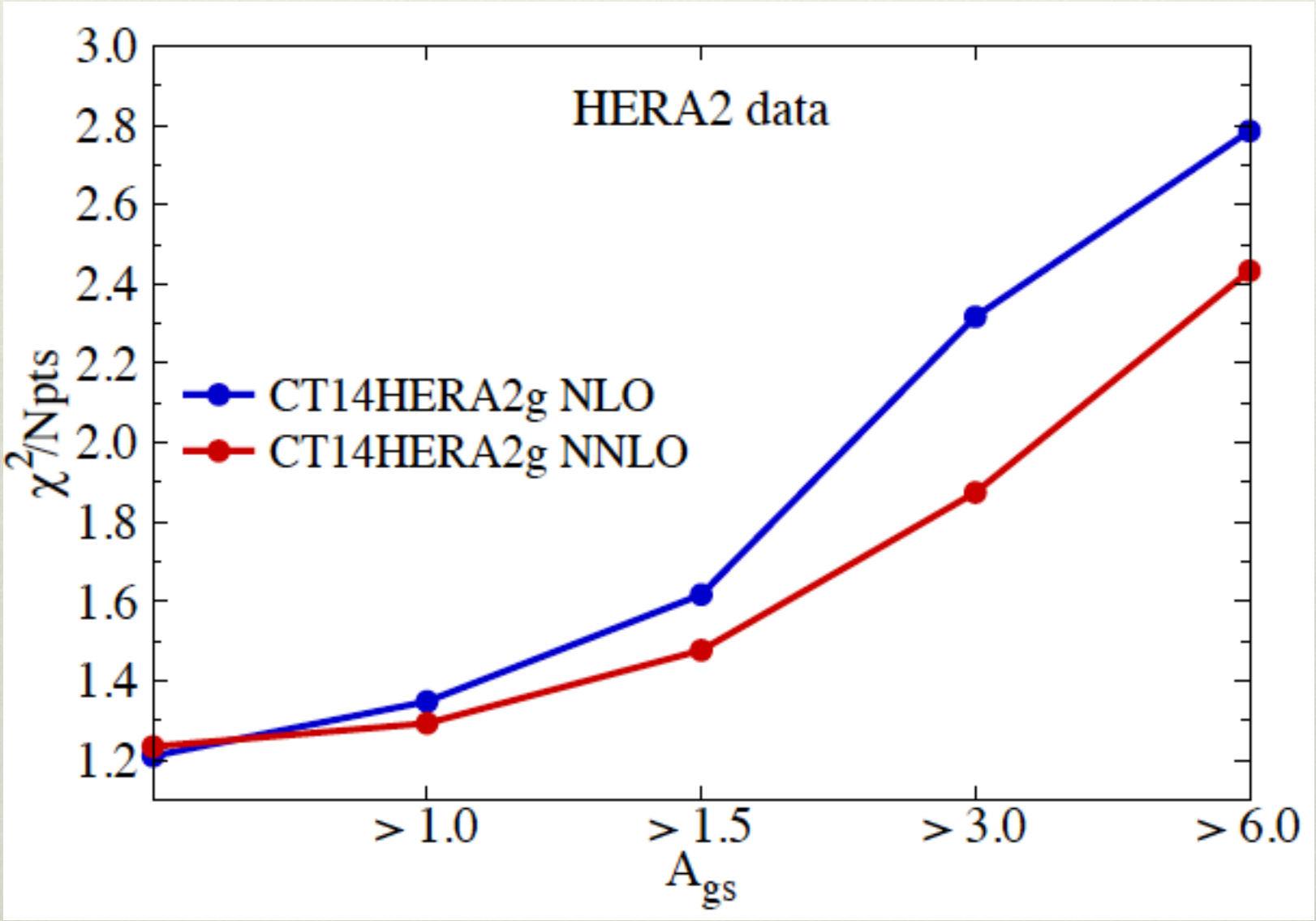
HERA2 data
CT14HERA2g NLO
CT14HERA2g NNLO
χ^2/Npts
3.0
2.8
2.6
2.4
2.2
2.0
1.8
1.6
1.4
1.2
> 1.0
> 1.5
> 3.0
> 6.0
A_{gs}